

Lattice dynamics of fcc helium at high pressure*

J. Eckert, W. Thomlinson, and G. Shirane

Brookhaven National Laboratory, Upton, New York 11973

(Received 7 April 1977)

The neutron-inelastic-scattering technique was used to measure the phonon dispersion relations in a high-density crystal of fcc He at 38 K. The crystal was grown at a pressure of 4.93 kbar and a temperature of 38.5 K in a high-pressure sample holder. Its lattice parameter was determined to be 3.915 ± 0.002 Å, equivalent to a molar volume of 9.03 cm³/mol. The measured dispersion curves were found to be in good agreement with a recent calculation by Goldman using the first-order self-consistent phonon theory without short-range correlation functions. The strong anharmonic effects observed in earlier measurements on the crystals of 21 cm³/mol were found to be much less prominent in this He crystal. The magnitude of the multiphonon interference effects on the one-phonon intensities is shown to be less than half of that observed in the low-density crystals. Thermodynamic analysis of the data yielded $\Theta_D^M = 154$ K which indicates that the ratio of mean amplitude of vibration to the nearest-neighbor distance is 8.6%, as opposed to nearly 30% for the lowest-density He crystals. The dependence of the phonon energies on volume is discussed with reference to the earlier work of Traylor *et al.* on an fcc crystal at 11.7 cm³/mol. Limited measurements were also made at 22 K to determine the temperature dependence of the phonon energies. Unusually large isochoric temperature shifts of as much as 15% for some phonons close to the zone center were found over the range of 22–38 K.

I. INTRODUCTION

The lattice dynamics of solid ⁴He may be considered to be reasonably well understood largely as a result of extensive theoretical activity prompted by the pioneering inelastic-neutron-scattering studies on the hcp,^{1–4} bcc,^{3–5} and fcc phases.⁶ The one-phonon response of the crystal when computed in some of the self-consistent lattice-dynamics theories gives generally good agreement with experiment, e.g., the work of Glyde and Khanna⁷ and of Horner⁸ on the bcc phase, the work of Gillis *et al.*⁹ on the hcp phase, and particularly the calculation of Horner⁸ on the fcc crystal studied by Traylor *et al.*⁶ More details on these and further calculations are contained in some recent review articles, e.g., those of Glyde¹⁰ and Koehler.¹¹

In addition to the one-phonon response several new and interesting features of the lattice dynamics of the highly anharmonic solid He emerged from the neutron-scattering studies: (i) the Q dependence of the observed intensities of the phonon groups was found to deviate strongly from that of the one-phonon harmonic-scattering cross section; (ii) some phonons measured at equivalent points in the reciprocal lattice not only had intensities which did not scale as expected but also had different peak positions, thus apparently destroying the symmetry of the reciprocal lattice; and (iii) liquidlike single-particle scattering was observed for large energy and momentum transfers. A satisfactory theoretical picture has emerged that describes these observations well. As a consequence of strong anharmonic interactions, multi-

phonon processes are frequently also excited by neutrons particularly at large Q and for large energy transfers. If such processes contain a single phonon as some intermediate state, they will contribute to the single-phonon scattering. These interference effects^{10, 12, 13} can affect the observed intensity and its peak position as will be discussed in more detail below (Sec. III B). The single-particle-like scattering at large Q may then be understood as being a superposition of multiphonon processes, since the linewidths indicate lifetimes for those processes to be determined by collisions between nearest neighbors.

Since solid He is expected to become more harmonic as the crystal is compressed and the equilibrium position of the He atom goes towards the bottom of the potential well, it was considered of interest to study the extent to which anharmonic effects are present in the high-density crystal. In addition to the study of the interference effects important information on the volume dependence of the phonon energies given by the Grüneisen parameters may be obtained by reference to the data of Traylor *et al.*⁶ Qualitative comparisons may also be made with the results on the hcp phase, where surprisingly the phonon energies of the two experiments at¹ 21.1 cm³/mol and² 16.0 cm³/mol were, with the exception of one branch, found to scale by a constant independent of wave vector.

Calculations of the volume dependence of the phonon energies should provide a stringent test of available theories, particularly on the way in which short-range correlations are treated. Both of the two standard approaches, i.e., Jastrow functions

and the T matrix,^{10, 11} result in too-small values of the Grüneisen parameter.¹⁰ Related to this problem is the question as to the density at which short-range correlations between the motions of the atoms are no longer important in describing the lattice dynamics of He. Horner¹⁴ has demonstrated that short-range correlations are important at densities as high as 11.5 cm³/mol, and his calculation⁸ which includes such effects does appear to give a better description of the phonon dispersion curves of Traylor *et al.*⁶ at 11.7 cm³/mol than that of Goldman *et al.*¹⁵ who used a cutoff of the hard core of the Lennard-Jones potential.

No information is available at present on another anharmonic effect, the isochoric temperature shift of the phonon energies in He. The reason for this is presumably that the temperature ranges of stability of the various phases of He at low densities are very small. This situation is greatly improved at high pressures, though the available temperature ranges are still small compared with those of other rare-gas solids.

In this paper, we describe a study of the lattice dynamics of a fcc He crystal at 9.03 cm³/mol. Following the description of the one-phonon response of the crystal, we will discuss multiphonon interference effects, temperature and volume shifts of the phonon energies, elastic properties, and zero-point motion in this high-density crystal.

II. EXPERIMENTAL DETAILS

The high-density He crystals used in this study were grown in a pressure cell at low temperature and high pressure in a manner most recently described in the work on solid Ne.¹⁶ The melting point of the crystal of 38.5 K and 4.93 kbar was chosen from the melting curve of Crawford and Daniels.¹⁷ Large single crystals which often filled more than half of the available sample holder volume of ~2.5 cm³ grew rather easily but frequently changed size and orientation upon annealing. A large crystal oriented with a $[\bar{1}\bar{1}2]$ axis approximately vertical was located after the crystal was cooled to 38 K. Its volume was estimated from the area of the diffracted beam to be ~1.3 cm³. In order to avoid the possibility of this crystal breaking up on further cooling most of the measurements were done at 38 K. Later the crystal was successfully cooled to 22 K, somewhat above the fcc-hcp phase transition, for limited measurements of the isochoric temperature shifts of the phonon energies.

Alignment of the $[\bar{1}\bar{1}2]$ zone allows measurements in the $[110]$ and $[111]$ symmetry directions only. A second crystal was therefore grown in a later experiment at the same density as the first to study the remaining $[100]$ branches. After some limited measurements were taken on this crystal

in a $[\bar{1}10]$ zone it was lost in an attempt to move the Dewar to a different spectrometer. Both crystals had mosaics of approximately 30-min full width at half maximum (FWHM). The positions of several Bragg peaks were used to determine the lattice parameter in both cases to be 3.915 ± 0.002 Å, corresponding to a molar volume of 9.03 cm³/mol.

The measurements of the phonon dispersion curves were done on triple-axis spectrometers at the Brookhaven High-Flux Beam Reactor, in the constant- Q mode of operation using fixed incident energies of 5, 13.7, and 14.8 meV or fixed final energy of 24 meV. A liquid-nitrogen-cooled Be filter was used to eliminate higher-order contamination of the 5-meV incident beam while pyrolytic graphite filters were used for the 13.7- and 14.8-meV beam. Monochromator and analyzer were pyrolytic graphite crystals, the former being cylindrically curved while the latter was flat. Horizontal-beam collimations of 20- or 40-min FWHM were used depending on energy and resolution requirements.

III. RESULTS AND DISCUSSION

A. Phonon dispersion relation at 38 K

Phonon groups typical of the high-resolution data used for the determination of the sound velocities are shown in Fig. 1. The solid line represents a fit to the data by one or two Gaussians with a linearly energy-dependent background. The peak positions thus obtained were corrected for slight shifts caused by instrumental resolution by a procedure most recently described by Fujii *et al.*¹⁸ This correction amounted to less than 2% in most cases but was as large as 10% for some phonons close to the zone center.

The corrected phonon energies are given in Table I. The errors shown are statistical as given by the Gaussian fitting procedure. Including systematic

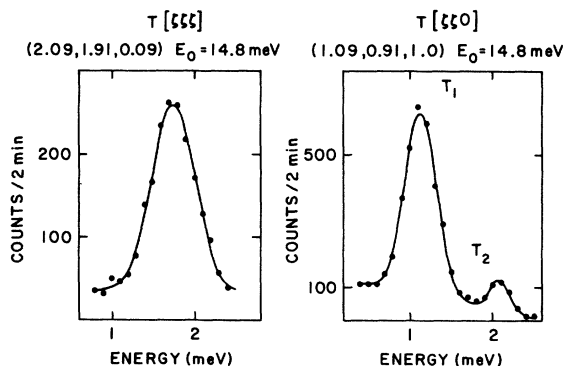


FIG. 1. Typical high-resolution phonon scans. Solid lines represent fitted Gaussians.

TABLE I. Experimental phonon energies for fcc He at $9.03 \text{ cm}^3/\text{mol}$ and 38 K. Errors given are statistical only. Overall errors are approximately 1.5 times as large.

ξ	[100]		[111]		[110]		L
	T	L	T	L	T ₁	T ₂	
0.025					0.305 ± 0.015		
0.03				1.56 ± 0.03	0.360 ± 0.010		
0.035					0.422 ± 0.010		
0.04				2.13 ± 0.05	0.482 ± 0.012		1.73 ± 0.03
0.05			0.972 ± 0.011	2.62 ± 0.01			2.11 ± 0.02
0.06			1.18 ± 0.01	3.15 ± 0.01	0.724 ± 0.018		2.44 ± 0.02
0.07			1.38 ± 0.02		0.824 ± 0.020	1.63 ± 0.02	
0.075				3.86 ± 0.12			
0.08	1.25 ± 0.01		1.57 ± 0.01		0.926 ± 0.010	1.87 ± 0.01	3.27 ± 0.02
0.09		2.31 ± 0.02	1.76 ± 0.01		1.06 ± 0.01	2.10 ± 0.01	3.72 ± 0.02
0.10	1.65 ± 0.01	2.56 ± 0.02	1.98 ± 0.01	5.09 ± 0.08	1.19 ± 0.01	2.31 ± 0.02	4.07 ± 0.04
0.11			2.14 ± 0.01				
0.125	1.99 ± 0.01	3.27 ± 0.02		6.29 ± 0.01	1.49 ± 0.01		
0.15	2.56 ± 0.02	3.80 ± 0.04	2.97 ± 0.05	7.55 ± 0.04	1.79 ± 0.02	3.48 ± 0.03	5.99 ± 0.08
0.2	3.24 ± 0.03		3.87 ± 0.04	9.88 ± 0.11	2.45 ± 0.02	4.70 ± 0.02	7.83 ± 0.14
0.25		6.41 ± 0.04	4.66 ± 0.15	12.51 ± 0.07			9.46 ± 0.11
0.3	4.69 ± 0.08		5.34 ± 0.06	14.05 ± 0.36	3.74 ± 0.03	7.05 ± 0.04	11.30 ± 0.13
0.35			5.67 ± 0.13				
0.4			6.19 ± 0.07		5.22 ± 0.05	9.21 ± 0.06	13.68 ± 0.28
0.5			6.63 ± 0.12		6.37 ± 0.10	10.81 ± 0.16	14.15 ± 0.24
0.6					7.77 ± 0.12		
0.7					9.03 ± 0.21		
0.8					9.96 ± 0.11		11.62 ± 0.16
0.9					10.81 ± 0.15		11.05 ± 0.10
0.95							11.01 ± 0.16
1.00					10.62 ± 0.14		10.62 ± 0.14

errors such as in the analyzer crystal setting the overall error in the phonon energies is estimated to be approximately 1.5 times the statistical errors in Table I. In cases where phonons at the

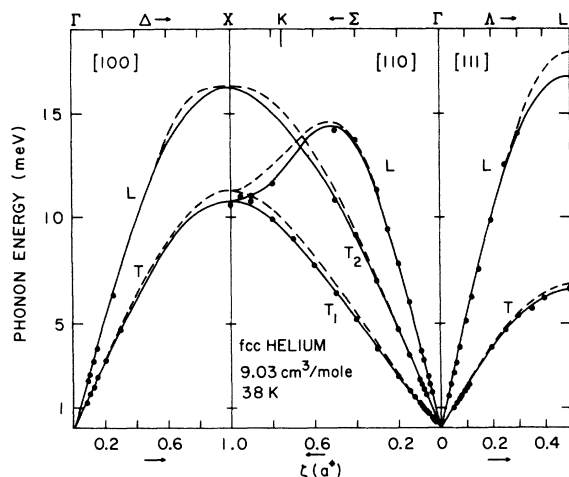


FIG. 2. Phonon-dispersion relations of high-density fcc He at 38 K and $9.03 \text{ cm}^3/\text{mol}$. Solid circles represent the resolution corrected measurements. Solid line is the fit given by a six-neighbor force constant model (Table II). Dashed line is the calculation of Goldman (Ref. 24).

same reduced wave vector ξ ($\xi = qa/2\pi$, where a is the lattice parameter) were measured at different points in reciprocal space or under different experimental conditions, appropriate averages are given, with the uncertainties adjusted to reflect the spread in observed values. The corresponding phonon-dispersion relations are shown in Fig. 2. Most of the experimental uncertainties are less than the size of the points plotted except for some of the higher-energy modes (see Table I). In addition, no well-defined peaks could be observed for some of the high-energy longitudinal [110] and [111] modes, as well as the T_2 [110] branch. Similar difficulties were encountered in the earlier work⁶ on fcc He at $11.7 \text{ cm}^3/\text{mol}$ as well as in studies of solid Ne at various densities.^{16, 19-21}

The solid line shown in Fig. 2 represents the fit of a Born-von Kármán force-constant model to the data, using a program developed by Svensson *et al.*²² The best representation of the experimental data was obtained by a model utilizing axially symmetric forces extending to sixth-nearest neighbors. No significance should be attached to the large number of neighbors used, or the individual numerical values of any of the force constants beyond those for nearest neighbors. The values for the force constants obtained in this fit are shown

TABLE II. Force constants for fcc He at $9.03 \text{ cm}^3/\text{mol}$ (dyn cm^{-1}). Column 1 shows the result of the fit to the data of a six-neighbor axially symmetric force-constant model. Column 2 shows force constants calculated in the harmonic approximation using 12-6 potential with $\epsilon = 10.22 \text{ K}$, $\sigma = 2.62 \text{ \AA}$.

Force constant	(1)	(2)
1XX	243 ± 9	250.0
1ZZ	-63 ± 5	-37.7
1XY	306 ± 11	287.7
2XX	10 ± 10	-1.2
2YY	4 ± 4	0.1
3XX	18 ± 5	0.3
3YY	7 ± 2	0.0
3YZ	4 ± 1	-0.1
3XZ	7 ± 3	-0.2
4XX	-4 ± 2	
4ZZ	-2 ± 4	
4XY	-2 ± 4	
5XX	-5 ± 2	
5YY	-1 ± 2	
5ZZ	0 ± 2	
5XZ	-2 ± 1	
6XX	-7 ± 2	
6YZ	-6 ± 2	

in Table II. For purposes of comparison we have also calculated force constants in the harmonic approximation using the improved Lennard-Jones 12-6 potential ($\epsilon = 10.22 \text{ K}$, $\sigma = 2.62 \text{ \AA}$) discussed by Hansen and Pollock.²³ Good agreement with experiment was obtained by these authors using this potential for the equation of state at $T = 0 \text{ K}$ computed by Monte Carlo methods. The calculated force constants surprisingly give excellent agreement with the experimental data. The resulting frequencies are generally slightly low, but disagree by no more than 6% with any measured phonon frequency. This agreement may be regarded as fortuitous, as a similar analysis in the work on solid Ne has shown.¹⁶ There it was found that the hard core radius σ of the 12-6 potential may be adjusted to yield force constants in agreement with experiment at a particular density. This scaling may be interpreted as reflecting the influence of zero-point motion, i.e., zero-point motion gives the atom a larger "effective" hard core. As the importance of zero-point motion decreases at higher densities the amount of scaling is reduced, until at some density the hard-core radius derived from gas data gives the appropriate force constants. This, therefore, would appear to be the case in the present study. Therefore, as far as the one-phonon energies are concerned, this crystal is quite harmonic.

The dashed line in Fig. 2 represents a calculation of phonon dispersion curves for this crystal

by Goldman.²⁴ The calculations were done utilizing the Beck potential in the self-consistent phonon theory of the form of Goldman *et al.*^{15, 25} which includes cubic anharmonicities but takes no account of short-range correlations (SC-1 in Ref. 25). The dispersion curves represent peaks of the one-phonon spectral function, neglecting multi-phonon interference terms. The agreement with the experimental data is very good, with the discrepancies for transverse modes at the zone boundary amounting to approximately 7%. This situation may be compared with the results for He at $11.7 \text{ cm}^3/\text{mol}$ studied by the Ames group. The calculation by Goldman *et al.*¹² resulted in higher frequencies towards the zone boundary with good initial slopes similarly to the present case. A somewhat different calculation by Horner which includes short-range correlations removes most of those discrepancies. Thus it may be concluded that short-range correlations could still be important at densities as high as $9 \text{ cm}^3/\text{mol}$. Further calculations are therefore definitely needed.

The force constants given in Table II were used to calculate the density of states by the method of Gilat and Raubenheimer²⁶ to allow the calculation of thermodynamic quantities. The result is shown in Fig. 3. The somewhat atypically large difference in energy between the critical points at $1\frac{1}{2}0$ (W point) and 100 (T point) may have been more substantiated if the point at $1\frac{1}{2}0$ had been measured.

Note should be made of the fact that the experimental data for the $[110] T_1$ branch shows a slight upward dispersion which appears to be reproduced in the calculation of Goldman.²⁴ Such results have been obtained in some calculations on both fcc and bcc He, notably in the self-consistent harmonic

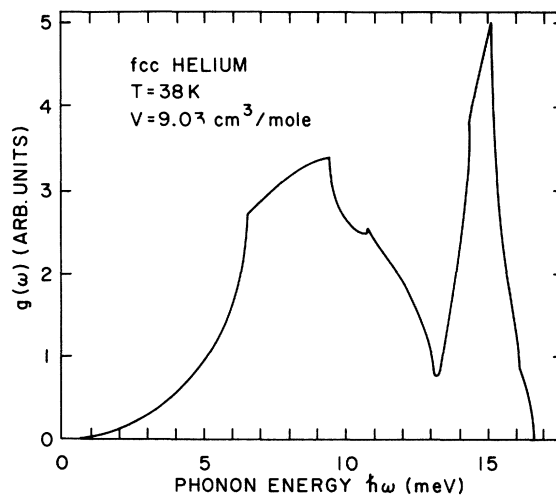


FIG. 3. Density of states for fcc He at 38 K and $9.03 \text{ cm}^3/\text{mol}$.

approximation¹⁰ and have therefore been regarded as artifacts of the type of approximation used.¹⁴ None of the previous data on the crystals reportedly showed any such anomaly. Such an upward dispersion should result in a specific-heat anomaly at low temperatures.¹¹ A calculation of $\Theta_D^C(T, V = V(38 \text{ K}))$ using the density of states computed from the force-constant model does indeed show a local maximum at $\sim 6 \text{ K}$. No appropriate thermodynamic data which should reflect this anomaly exists for this density. However, specific-heat data at volumes down to $13.7 \text{ cm}^3/\text{mol}$ by Ahlers²⁷ in the hcp phase do not show any such anomaly.

The natural widths of the phonon groups were also determined in the above data analysis. They were taken as the difference in the squares of the observed FWHM as determined from the Gaussian fits to the experimental data and the computed FWHM resulting from the instrumental line-shape calculation by the method of Werner and Pynn.²⁸ The results are shown in Fig. 4. The results are shown in Fig. 4. The error bars indicated are a combination of the statistical error given by the Gaussian fits to the experimental data and an assumed 5% uncertainty in the instrumental resolution. While the uncertainties in this determination are rather large, these results nevertheless give a definite trend of broadening away from the zone center for both longitudinal and transverse modes.

B. Multiphonon interference effects

Previous studies of solid He in its hcp and bcc phases^{1, 4, 5} at low densities have revealed strong anomalies of the apparent Debye-Waller factor as determined from the intensities of the observed scattering, as well as pronounced asymmetric line shapes for some phonons. The Debye-Waller factor W is determined from the sum rule developed by Ambegaokar *et al.*,²⁹ i.e.,

$$M^1 \equiv \int_{-\infty}^{\infty} \frac{d\omega}{2\pi} \omega S_p(\vec{Q}, \omega) = \frac{\hbar}{2M} (\vec{Q} \cdot \vec{\xi})^2 e^{-2W}, \quad (1)$$

where $S_p(\vec{Q}, \omega)$ is the scattering function for scattering by one-phonon as well as multiphonon processes which have a single phonon as some intermediate stage. The scattering cross section for creation of a single phonon of frequency, $\omega_j(q)$ in a constant- \vec{Q} scan is given by³⁰

$$\sigma \propto [n_j(\vec{q}) + 1] \{ [\vec{Q} \cdot \vec{\xi}_j(\vec{q})]^2 / \omega_j(\vec{q}) \} e^{-2W}, \quad (2)$$

where $n_j(\vec{q})$ is the phonon occupation number, and $\vec{\xi}_j(\vec{q})$ is the polarization vector of the phonon. Thus, W may be obtained from the intensities of the observed neutron groups by plotting the quantity $\ln[M^1/(\vec{Q} \cdot \vec{\xi})^2]$ as a function of Q^2 . In the harmonic

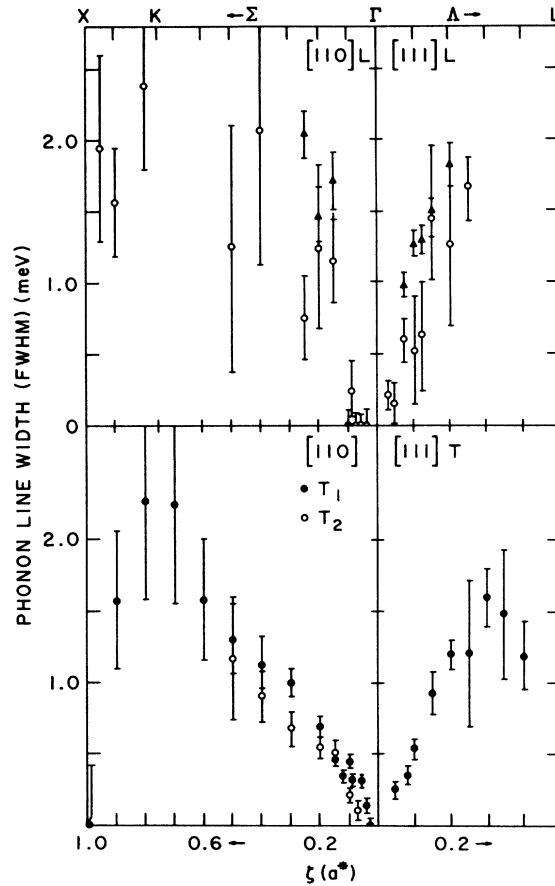


FIG. 4. Natural widths of observed phonon groups. For reasons of clarity not all data are shown.

approximation W is a Gaussian function of $|\vec{Q}|$, and this plot gives a straight line of slope W . The observations^{1, 4, 5} in the work on bcc and hcp He amounted therefore to large oscillations of the perceived Debye-Waller factor around its harmonic value.

The explanation for the experimental observation lies in the realization that $S_p(\vec{Q}, \omega)$ in Eq. (1) includes interference terms between one-phonon and multiphonon processes. Werthamer,³¹ Beck and Meier,³² and Horner¹² first demonstrated how inclusion of the leading interference term, that between one- and two-phonon processes, in the line-shape calculations could account for the experimental observations. More recently, Glyde¹⁴ explicitly demonstrated the effects of the interference terms on observed phonon line shapes. The first contribution is to the intensity of the one-phonon peak. It is symmetric with respect to that peak and its sign depends on the sign of \vec{q} with respect to the nearest Bragg point. The second contribution gives an asymmetric contribution to the background of the one-phonon peak. Only if the in-

trinsic linewidth of the phonon is relatively large will this term result in pronounced asymmetric line shapes. If so, the apparent peak position may shift, so that identical phonons measured on both sides of a Bragg point may appear to have different energies. This effect was clearly observed in bcc helium.^{4,5}

Such interference effects, though most pronounced in highly anharmonic low-density He crystals, have also been observed in other systems, most recently in K by Meyer *et al.*³³ In a careful study, these authors were able to demonstrate the symmetric term as relatively small oscillations around the harmonic Debye-Waller factor. The asymmetric term was found to only affect the slopes of the

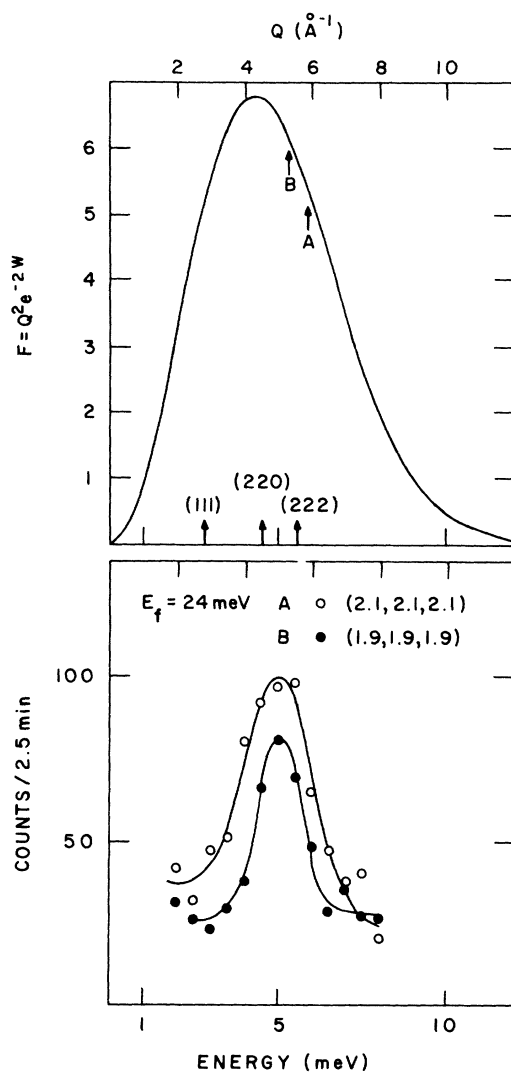


FIG. 5. Top part indicates normal Q dependence of the single phonon cross section for solid He with $\Theta = 154$ K. The bottom shows two phonon groups measured at equivalent positions in reciprocal space.

background on either side of the Bragg point, but not to distort the line shapes of the phonons noticeably. At low temperatures, anharmonic effects in such systems as K are much reduced. Thus, no significant departure from harmonic behavior of the Debye-Waller factor was found at 4.2 K.

It was therefore of interest to study to what extent interference effects might be present in high-density He compared with previous results. Figure 5 shows phonon groups for the $L[111]$ mode of $\zeta = 0.1$ measured at equivalent points on both sides of the 222 Bragg point. The upper half of Fig. 5 indicates how one would expect the intensities of the two peaks to scale, i.e., it should be proportional to $Q^2 e^{-2W}$. The integrated intensity of the peak at $\zeta = +0.1$ is approximately 50% larger than that of the peak at $\zeta = -0.1$ whereas one would expect it to be some 15% lower from consideration of Fig. 5. A similar plot was shown in the work on bcc He for a different phonon,⁴ displaying a discrepancy more than twice as large as in the current case. From these considerations one may conclude that the effect of the symmetric interference term in the high-density crystal has been reduced by about a factor of two over that in bcc He.

More generally, one can display the influence of the symmetric interference term as oscillations about the harmonic Debye-Waller factor. Shown in Fig. 6 is the quantity $\ln[M^1/(\vec{Q} \cdot \vec{\xi})^2]$ plotted vs Q^2 for both the $[110]$ and $[111]$ directions. The slope of this line is given by the Debye-Waller factor [Eq. (1)], where we have used $\Theta_D^M = 154$ K as computed from the density of states and experimental intensities obtained by integrating the area under the fitted Gaussian. We have included only data taken under identical experimental conditions and only if intensities could be determined with reasonable accuracy. The dashed line drawn in Fig. 6 is merely intended to be a guide to the eye. It reflects the theoretical result that the symmetric interference term vanishes at reciprocal lattice points and at midpoints between reciprocal-lattice points.¹³ In general, the data clearly show the expected oscillation in the vicinity of the Bragg points while not enough data are available to clearly demonstrate the behavior of the interference term between Bragg points. The amplitude of the oscillation about the harmonic Debye-Waller factor is approximately 50%, i.e., the highest (lowest) points in the curve are $\sim 50\%$ higher (lower) than the value given by the straight line. In the case of bcc He (Fig. 12 of Ref. 4) the amplitude of the oscillations is more than twice as large.

While the symmetric interference term is therefore still very much in evidence in this high-density fcc He crystal, the asymmetric contri-

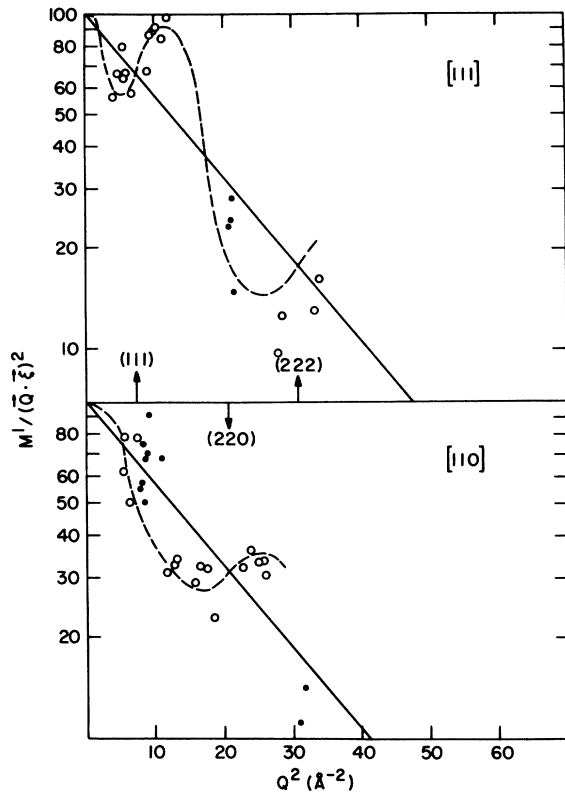


FIG. 6. Effective Debye-Waller factor for fcc He for the [110] and [111] directions. Longitudinal modes are indicated by open circles, transverse modes by closed circles. Dashed line is drawn to reflect the expectations of the theory (Ref. 13) and is a guide to the eye only.

bution was not nearly as clear as in bcc He. Strongly asymmetric phonon line shapes (Fig. 3 of Ref. 4) were observed with different apparent peak positions for phonons measured at equivalent points in reciprocal space. With the exception of some of the high-energy longitudinal modes non-Gaussian line shapes were not observed in this high-density fcc He crystal. However, phonons measured at equivalent points on either side of a Bragg point did have noticeably different background slopes. This then may be taken as the manifestation of the asymmetric interference term, as is predicted¹³ for cases where the phonon is not substantially broadened.

In the brief study of phonons at 22 K (see Sec. III C) interference effects were still found to be present, though reduced from those at 38 K. A more extensive study of phonons at 22 K could give valuable information on the temperature dependence of the interference terms.

C. Isochoric temperature shifts

The technique used in this experiment for growing crystals from the melt directly at high densi-

ties and low temperatures has the advantage that phonon energies can be studied as a function of temperature at constant volume, as the pressure cell is much stiffer than van der Waals solids such as He. Thus the anharmonic temperature shift is not obscured by the generally much larger quasiharmonic volume shift of the phonon energies. In a study on solid Ne at 13.3 cm³/mol, Skalyo *et al.*²⁰ determined shifts of as much as $\sim -3.5\%$ for transverse [100] phonons from 5 to 22 K and shifts in the order of $\sim +2\%$ for longitudinal [100] modes. The shifts tended to become more positive in going from the zone center towards the zone boundary. A calculation by Koehler³⁴ accounts fairly well for similar results obtained earlier by Leake *et al.*¹⁹ on a Ne crystal at 12.86 cm³/mol. A more recent calculation by Goldman and Klein using an improved Ne-Ne potential also reproduces the observed temperature dependence fairly well.³⁵

In addition to the extensive measurements at 38 K described above we have also performed limited measurements at 22 K under an identical set of experimental conditions. No change in the lattice parameter could be determined within experimental accuracy. Shown in Table III are the limited results obtained at 22 K along with the computed temperature shifts. While these shifts show a similar q dependence to the results on solid Ne,^{19,20} the magnitude of the shifts, particularly for the transverse modes, is unexpectedly large. Furthermore, the shifts for the longitudinal modes

TABLE III. Isochoric temperature shifts in fcc helium, 9.03 cm³/mol. % shift $\equiv [E(38 \text{ K}) - E(22 \text{ K})]/E(22 \text{ K})$.

ξ	$E(22 \text{ K})$	$E(38 \text{ K})$	% shift
$T_1[110]$			
0.07	0.973 \pm 0.010	0.824 \pm 0.020	-15.3 \pm 2.2
0.08	1.07 \pm 0.01	0.926 \pm 0.010	-13.5 \pm 1.3
0.09	1.25 \pm 0.01	1.06 \pm 0.01	-15.2 \pm 1.1
0.125	1.71 \pm 0.01	1.49 \pm 0.01	-12.9 \pm 0.9
0.15	2.04 \pm 0.01	1.79 \pm 0.02	-12.3 \pm 1.2
0.2	2.75 \pm 0.02	2.45 \pm 0.02	-10.9 \pm 1.0
$T_2[110]$			
0.07	1.72 \pm 0.01	1.63 \pm 0.02	-5.2 \pm 1.3
$L[110]$			
0.08	3.40 \pm 0.02	3.27 \pm 0.02	-3.8 \pm 0.8
$T[111]$			
0.06	1.34 \pm 0.01	1.18 \pm 0.01	-11.9 \pm 1.0
0.08	1.76 \pm 0.01	1.57 \pm 0.01	-10.8 \pm 0.7
0.11	2.37 \pm 0.01	2.14 \pm 0.01	-9.7 \pm 0.7
$L[111]$			
0.03	1.62 \pm 0.04	1.56 \pm 0.03	-3.7 \pm 3.0
0.05	2.69 \pm 0.05	2.62 \pm 0.01	-2.6 \pm 1.8

are also negative, while both experiment and theory show positive shifts in the Ne case mentioned above. It is unlikely that standard self-consistent theories could predict a temperature shift of the magnitude shown here.²⁴ Clearly, a more extensive study at 22 K is required to obtain further information on the temperature shift and its q dependence.

D. Compression dependence of phonon energies

In this section, we present a comparison between the present results and those of the Ames group on an fcc He crystal at 11.7 cm³/mol and 15.5 K.⁶ It should be pointed out that in the following discussion the temperature dependence of the phonon energies has been neglected. Comparisons should, however, still be valid, since both experiments were carried out near their respective melting temperatures.

The volume dependence of the phonon frequency $\omega_j(\vec{q})$ is given by the mode Grüneisen parameter $\gamma_j(\vec{q}) = -d \ln \omega_j(\vec{q}) / d \ln V$. In principle, the $\gamma_j(\vec{q})$ may all be different for different modes. Furthermore, $\gamma_j(\vec{q})$ may itself depend on volume. Table IV shows the mode Grüneisen parameters that were calculated by comparing data with those of Traylor *et al.*⁶ wherever the same phonon was measured. Since a possible volume dependence of the mode Grüneisen parameter is a higher-order effect, it is neglected. The uncertainties listed in Table IV reflect the combined errors in the phonon energies

TABLE IV. Volume shifts of phonon energies from $V_1 = 11.72$ (data of Ref. 6) to 9.03 cm³/mol.

ξ	E_1	E_2	$\gamma_i(\vec{q})$
T[100]			
0.2	2.07 ± 0.21	3.24 ± 0.03	1.72 ± 0.45
0.3	2.94 ± 0.04	4.69 ± 0.08	1.79 ± 0.14
T[110]			
0.3	2.40 ± 0.04	3.74 ± 0.03	1.70 ± 0.12
0.4	3.35 ± 0.08	5.22 ± 0.05	1.70 ± 0.15
0.5	4.01 ± 0.08	6.37 ± 0.10	1.77 ± 0.15
0.6	4.76 ± 0.16	7.77 ± 0.12	1.88 ± 0.20
0.7	5.38 ± 0.12	9.03 ± 0.21	1.99 ± 0.18
0.8	5.79 ± 0.12	9.96 ± 0.11	2.08 ± 0.15
0.9	6.04 ± 0.12	10.81 ± 0.15	2.23 ± 0.16
1.0	6.20 ± 0.12	10.62 ± 0.14	2.06 ± 0.15
L[110]			
0.2	4.71 ± 0.08	7.83 ± 0.14	1.94 ± 0.15
0.3	6.62 ± 0.08	11.30 ± 0.13	2.05 ± 0.13
0.4	7.73 ± 0.21	13.68 ± 0.28	2.19 ± 0.20
0.8	6.78 ± 0.08	11.62 ± 0.16	2.07 ± 0.13
0.9	6.48 ± 0.08	11.05 ± 0.10	2.05 ± 0.12

as presented in Table I and Table I of Traylor *et al.*⁶

While the error associated with each mode Grüneisen parameter is in some instances quite large, there is nevertheless significant variation throughout the zone. However, the data are not complete enough to make detailed comparisons with the results on Ne by Eckert *et al.*,¹⁶ who presented complete dispersion relations for mode Grüneisen parameters for the principal symmetry directions. One may, however, point out that the difference in mode "gammas" between transverse and longitudinal modes seems to be larger in Ne than in fcc He.

While no further information is available on Grüneisen parameters in fcc He, an analysis was presented by Reese *et al.* of their study of phonon frequencies in hcp He at 16.0 cm³/mol² as compared with that of Minkiewicz *et al.*¹ at 21.1 cm³/mol. Their conclusion was that all frequencies scaled by approximately the same factor of 1.9. However, a late study of the LO [001] branch in hcp He by Minkiewicz *et al.*,⁴ which had not been observed in their earlier work¹ yielded a scale factor of 2.6 ($\gamma \sim 3.0$). The suggestion was made by Minkiewicz *et al.*¹⁴ that this difference may be the result of a possibly incorrect assignment of phonon energies for the LO [001] branch by Reese *et al.*² due to multiphonon scattering effects. A recent study of Raman scattering from the TO mode at the zone center in hcp He at various densities up to ~ 17 cm³/mol yielded $\gamma_t = 2.6 \pm 0.1$.³⁶ One may therefore conclude that the initial result of Reese *et al.*² of a uniform scaling with volume of the phonon energies for all modes in hcp He may indeed not exist.

The two sets of data^{1,2} on hcp He were also analyzed by Reese *et al.*² for a possible volume dependence of γ . On assuming a linear dependence of γ on volume this analysis leads to the conclusion that $\gamma = 2.66$ at 21.1 cm³/mol and $\gamma = 2.02$ at 16.0 cm³/mol, approximately the same for all modes. While it may be inappropriate to compare mode gammas in the hcp and fcc phases, the numbers presented in Table IV for the range 9.03 cm³/mol to 11.72 cm³/mol suggest that the volume dependence obtained by Reese *et al.*² is likely to be too strong. This conclusion may be supported by the results of Ahlers²⁷ on the thermodynamic Grüneisen parameter γ_G in hcp He. He obtained a much weaker volume dependence, i.e., $\gamma_G = 1.02 + 0.083V$ over the range $V = 13.7$ to 20.8 cm³/mol. For $V = 9.03$ cm³/mol this result yields $\gamma_G = 1.77$. While γ_G is an average of the mode gammas over the Brillouin zone its value will be mainly determined by the low-lying transverse modes, which are shown in Table IV to have values close to this γ_G .

E. Elastic properties

Zero-sound elastic constants may be obtained in measurements of phonon dispersion relations both directly from the sound velocities and from the force constants determined in the fitting procedure. In the former case, a sufficient amount of high-resolution data at small wave vector has to be taken to accurately determine the initial slopes of the dispersion curves. In the latter case, elastic constants are obtained as linear combinations of the interatomic force constants. A commonly used indicator for the extent of zero-point motion is the degree to which the Cauchy relation is satisfied. For an fcc crystal at $T = 0$ K under no external pressure with central forces only and no zero-point motion the deviation from the Cauchy relation

$$\delta = (C_{44}^* - C_{12}^*)/C_{12}^* \quad (3)$$

is equal to zero. Elastic constants measured under external pressure P must be adjusted by using the relationships³⁷

$$C_{11}^* = C_{11} + P, \quad C_{44}^* = C_{44} + P, \quad C_{12}^* = C_{12} - P, \quad (4)$$

where the unstarred quantities are the measured values. Inclusion of zero-point motion is known to make C_{44}^* slightly larger than C_{44} , while with increasing temperature C_{12}^* becomes larger than C_{44}^* .

Shown in Table V are the elastic constants and related quantities obtained by both methods referred to above. The value used in correcting the elastic constants for pressure is the melting pressure as determined from the melting curve of Crawford and Daniels, i.e., 4.93 kbar. An uncertainty of ± 0.1 kbar in the pressure resulting from a somewhat uncertain temperature profile in the cell during growth and the fact that the measurement was performed 0.5 K below the melting point was included in the errors given for the elastic constants.

TABLE V. Elastic constants (10^8 dyn cm⁻²) and associated parameters for fcc He at 38 K and 9.03 cm³/mol. $B_0 = \frac{1}{3}(C_{11}^* + 2C_{12}^*)$ in units of 10^8 dyn cm⁻², $A = 2C_{44}^*/(C_{11}^* - C_{12}^*)$, and $\delta = C_{44}^* - C_{12}^*/C_{12}^*$. (1) From force constant model of Table I. (2) Result of fitting sound velocities directly.

	(1)	(2)
C_{11}^*	307 \pm 3	308 \pm 4
C_{12}^*	156 \pm 3	155 \pm 5
C_{44}^*	155 \pm 2	156 \pm 3
A	2.05 \pm 0.06	2.04 \pm 0.07
B_0	206.3 \pm 2	206.0 \pm 3
δ	$\sim 0 \pm 0.02$	$\sim 0 \pm 0.02$

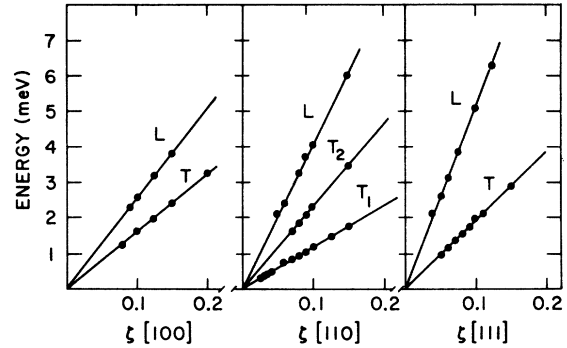


FIG. 7. Initial slopes of the dispersion curves used in deriving sound velocities. Lines are the result of a single-parameter fit.

The initial slopes of the dispersion curves may be fitted to the relationship

$$\hbar\omega = E_0 + V_s q + Bq^3, \quad (5)$$

where E_0 allows for systematic error in the analyzer setting, and B accounts for a possible non-linearity in the dispersion relation. V_s is the sound velocity for a particular branch, and its relationship to the elastic constant is used for their determination. In no case, however, could either E_0 or B be determined with sufficient precision from the fitting procedure. Therefore, sound velocities obtained from one parameter fits of the linear term only were used to derive the elastic constants given in column 2 of Table V. The agreement with those obtained from the force constant model is excellent. The long-wavelength portions of the dispersion relations used in this procedure are shown in Fig. 7.

Note may be made of the fact that these elastic constants satisfy the Cauchy relation, Eq. (3), to within experimental error. In view of the comments made above, this result should be understood as an accidental cancellation of the effects on δ of zero-point motion and thermal energy at this particular experimental temperature. An indication of the degree of importance of zero-point motion may, however, be inferred from the ratio of the root of the mean amplitude squared of vibration, $\frac{1}{3} < u^2 >$, to the nearest-neighbor distance. Using the value $\Theta_D^M(T = 38 \text{ K}) = 154 \text{ K}$ calculated from the density of states one obtains a ratio of 8.6%. At the lowest density of solid He this ratio is close to 30%, while for Ne at 1 atm it is 5.1% at low temperatures and increases to 6.5% just below the melting point.¹⁹ Thus the relative importance of zero-point motion in the present high-density crystal is greatly reduced from that of previously studied He crystals, as was also demonstrated in the discussion on multiphonon effects

above. Similarly, a more complete study at 22 K should, on the basis of these considerations and the limited measurements of this experiment, show further reduction in the magnitude of anharmonic effects such as multiphonon interference effects.

IV. CONCLUDING REMARKS

Results of this neutron-scattering study on a fcc He crystal at $9.03 \text{ cm}^3/\text{mol}$ show the same anharmonic effects, though much reduced in magnitude, as did previous studies on crystals at much lower densities.¹⁻⁵ In addition, a large isochoric temperature shift of the phonon energies over the limited temperature range 22–38 K was observed. More extensive measurements of this effect are clearly required, as the magnitude of this shift is somewhat unexpected. In order to obtain a more detailed q dependence of mode Grüneisen parameters than was possible in this work with reference to the limited data of Traylor *et al.*⁶ studies on fcc crystals of lower densities are in progress at this laboratory. In addition, measurements on high

density hcp He crystals are in progress, which in conjunction with the two previous measurements¹⁻⁴ should yield detailed information on the compression dependence of phonon energies in the hcp phase as well, where more thermodynamic measurements are available for comparison. Finally, it may be of interest to extend these measurements to still higher densities. There has been a calculation of the He phase diagram by a Monte Carlo calculation by Holian *et al.*³⁸ suggesting that at pressures above $\sim 15 \text{ kbar}$ the fcc phase will be stable down to $T = 0 \text{ K}$. As solid He becomes more harmonic at higher densities this would indeed be expected to happen. Measurements at those pressures may therefore prove of interest.

ACKNOWLEDGMENTS

We would like to thank V. V. Goldman for sending us the results of his calculation prior to publication, and H. R. Glyde and V. V. Goldman for useful discussions.

*Work performed under the auspices of the U. S. ERDA.

¹V. J. Minkiewicz, T. A. Kitchens, F. P. Lipschultz, R. Nathans, and G. Shirane, *Phys. Rev.* **174**, 267 (1968).

²R. A. Reese, S. K. Sinha, T. O. Brun, and C. R. Tilford, *Phys. Rev. A* **3**, 1688 (1971).

³T. A. Kitchens, G. Shirane, V. J. Minkiewicz, and E. B. Osgood, *Phys. Rev. Lett.* **29**, 552 (1972).

⁴V. J. Minkiewicz, T. A. Kitchens, G. Shirane, and E. B. Osgood, *Phys. Rev. A* **8**, 1513 (1973).

⁵E. B. Osgood, V. J. Minkiewicz, T. A. Kitchens, and G. Shirane, *Phys. Rev. A* **5**, 1537 (1972).

⁶J. G. Traylor, C. Stassis, R. A. Reese, and S. K. Sinha, in *Inelastic Scattering of Neutrons* (IAEA, Vienna, 1972).

⁷H. R. Glyde and F. C. Khanna, *Can. J. Phys.* **50**, 1143 (1972).

⁸H. Horner, *J. Low Temp. Phys.* **8**, 511 (1972).

⁹N. S. Gillis, T. R. Koehler, and N. R. Werthamer, *Phys. Rev.* **175**, 1110 (1968).

¹⁰H. R. Glyde, in *Rare Gas Solids*, Vol. I, edited by M. L. Klein and J. A. Venables (Academic, New York, 1976).

¹¹T. R. Koehler, in *Dynamical Properties of Solids*, edited by G. K. Horton and A. A. Maradudin (North-Holland, Amsterdam, 1975).

¹²H. Horner, *Phys. Rev. Lett.* **29**, 556 (1972).

¹³H. R. Glyde, *Can. J. Phys.* **52**, 2281 (1974).

¹⁴H. Horner, *Solid State Commun.* **9**, 79 (1971).

¹⁵V. V. Goldman, G. K. Horton, and M. L. Klein, *Phys. Rev. Lett.* **24**, 1424 (1970).

¹⁶J. Eckert, W. B. Daniels, and J. D. Axe, *Phys. Rev. B* **14**, 3649 (1976).

¹⁷R. K. Drawford and W. B. Daniels, *J. Chem. Phys.* **55**, 5651 (1971).

¹⁸Y. Fujii, N. A. Lurie, R. Pynn, and G. Shirane, *Phys. Rev. B* **10**, 3647 (1974).

¹⁹J. A. Leake, W. B. Daniels, J. Skalyo, Jr., B. C. Frazer, and G. Shirane, *Phys. Rev.* **181**, 1251 (1969).

²⁰J. Skalyo, Jr., V. J. Minkiewicz, G. Shirane, and W. B. Daniels, *Phys. Rev. B* **6**, 4766 (1972).

²¹Y. Endoh, G. Shirane, and J. Skalyo, Jr., *Phys. Rev. B* **11**, 1681 (1974).

²²E. C. Svensson, B. N. Brockhouse, and R. M. Rowe, *Phys. Rev.* **155**, 619 (1967).

²³J. P. Hansen and E. L. Pollock, *Phys. Rev. A* **5**, 2651 (1972).

²⁴V. V. Goldman (private communication).

²⁵H. R. Glyde and V. V. Goldman, *J. Low Temp. Phys.* **25**, 601 (1976).

²⁶G. Gilat and R. J. Raubenheimer, *Phys. Rev.* **144**, 390 (1966).

²⁷G. Ahlers, *Phys. Rev. A* **2**, 1505 (1970).

²⁸R. Pynn and S. A. Werner, Laboratory Report No. AE-FF-112 (A. B. Atomenergi, Studsvik, Sweden) (unpublished); S. A. Werner and R. Pynn, *J. Appl. Phys.* **42**, 4736 (1971).

²⁹V. Ambegaokar, J. M. Conway, and G. Baym, *J. Phys. Chem. Solids Suppl.* **1**, 261 (1965); in *Proceedings of the International Conference on Lattice Dynamics* (Pergamon, New York, 1965).

³⁰B. N. Brockhouse and P. K. Iyengar, *Phys. Rev.* **111**, 747 (1958).

³¹N. R. Werthamer, *Phys. Rev. Lett.* **28**, 1102 (1972).

³²H. Beck and P. F. Meier, *Phys. Kondens. Mater.* **14**, 336 (1972).

³³J. Meyer, G. Dolling, R. Scherm, and H. R. Glyde, *J. Phys. F* **6**, 943 (1976).

³⁴T. R. Koehler, *Phys. Rev. Lett.* **22**, 777 (1969).

³⁵V. V. Goldman and M. L. Klein, *J. Low Temp. Phys.* 22, 501 (1976).

³⁶R. E. Slusher and C. M. Surko, *Phys. Rev. B* 13, 1086 (1976).

³⁷T. H. K. Barron and M. L. Klein, *Proc. Phys. Soc. Lond.* 85, 523 (1965).

³⁸B. L. Holian, W. D. Gwinn, A. C. Luntz, and B. J. Alder, *J. Chem. Phys.* 59, 5444 (1973).